Hybrid Genetic Programming for the Development of Metamaterials Designs With Improved Characteristics

Scott Clemens, *Member, IEEE*, Magdy F. Iskander, *Life Fellow, IEEE*, Zhengqing Yun, *Member, IEEE*, and Jennifer Rayno, *Member, IEEE*

***Abstract*—The expansion of a hybrid genetic program's (HGP) functionality to allow for the development of broadband two-dimensional metamaterials designs with advanced characteristics is presented. Artificial magnetic conductor (AMC) ground planes and a tunable terahertz absorber generated by the HGP are compared with designs available in the literature. The HGP is shown to produce human-competitive results. The AMC ground planes synthesized by the HGP were found to produce improved results including wider bandwidths and larger reflection coefficient magnitudes than that of the human designs. For one of the designed AMCs, the HGP's bandwidth is 73.3% larger and the minimum reflection magnitude is 1.0% larger than the reference AMC. Similarly, the absorber synthesized by the HGP has larger bandwidths than that of a recently published absorber optimized by random hill climbing. Three bias voltages were tested with the tunable absorber. The bandwidths of the HGP absorber are 23.1%, 37.6%, and 400% larger than the reference absorber, for biases of 4, 2, and 0.5 V/nm, respectively. Four example designs are discussed together with comparative results to illustrate the advantages of the developed HGP-enabled design method.**

***Index Terms*—Artificial magnetic conductor (AMC), genetic algorithm (GA), genetic programming (GP), terahertz (THz) absorber.**

I. Introduction

METAMATERIALS are artificial structures that have properties not found in natural materials [1]. For example, artificial magnetic conductors (AMCs), a subclass of metamaterial structures, can behave as perfect magnetic conductors (PMCs) over selected frequency bands. A PMC has an in-phase total reflection and can be used as a ground plane to be placed much closer to an antenna than the frequency-dependent spacing typically used with perfect electric conductor (PEC) ground planes. This results in low-profile antenna designs while providing higher gain over a relatively broadband of operation.

Metamaterials can also be designed to fill in the terahertz (THz) gap where natural materials have weaker electromagnetic responses, as THz range lies between the lower frequencies where electrons are the primary particle that devices utilize and the higher frequencies where photons become the primary particle [2]. Many THz absorber designs have been reported in the literature, with applications in imaging [3], [5], sensing [2], [6], stealth [7], and communication [8], and interest continues to grow in designing new metamaterials to support these applications.

Work has been done to improve the design process of AMC ground planes, and optimization algorithms such as genetic algorithms (GAs) have proven to be successful in creating ground planes that exhibit desirable qualities, such as low profile, low loss, and/or multiband operation [9]–[11]. The implementation of genetic programming (GP) has also been explored with success [12], [13]. In [13], successful three-dimensional (3-D) generated AMC designs with broadband characteristics were reported, and in [14], a hybrid genetic program (HGP) that utilizes GA as a low-level optimizer to speed up the computational process has been successfully implemented. In this letter, the HGP code has been expanded to include the development of 2-D metamaterials designs with advanced characteristics. Specifically, while the developed HGP in [14] has been used to design AMC ground planes in the 225–450 MHz range, thus covering the high VHF and low UHF bands, it was difficult to fabricate and experimentally test the produced designs. By expanding the capabilities of the HGP to allow for 2-D designs that could be fabricated and tested, more verification of the GP design methodology will be possible and interest in this advanced design method would continue to grow and help address needs in variety of EM research areas. In this letter, we chose a 2-D design space in the 3–30 GHz band for its relative fabrication ease and low-cost prototyping. For this study, 2-D metamaterial AMC and THz absorbers designs that are available in the literature were used for reference, and new designs were synthesized using the new HGP code. Obtained results show that the GP code could produce designs with superior performance than those published earlier. For the THz absorbers case, we also compared the GP results with yet another recently published evolutionary-inspired optimization technique [15]. It is shown that GP did provide designs of broader bandwidth than those of the THz absorbers in [15].

In Section II, we describe the 2-D AMC and THz absorber implementations of the HGP code, while in Section III we describe and compare results for the AMCs and THz absorber generated by the HGP with designs reported in the literature. Section IV includes concluding remarks.

Manuscript received November 24, 2017; revised December 31, 2017; accepted January 11, 2018. Date of publication January 31, 2018; date of current version March 1, 2018. This work was supported by the National Science Foundation under Grant ECCS-1304917. *(Corresponding author: Magdy F. Iskander.)*

The authors are with Hawaii Center for Advanced Communications, University of Hawaii at Manoa, Honolulu, HI 96822 USA (e-mail: scottkc@hawaii.edu; magdy.iskander@gmail.com; zyun@hawaii.edu; jrayno@hawaii.edu).

Digital Object Identifier 10.1109/LAWP.2018.2800057

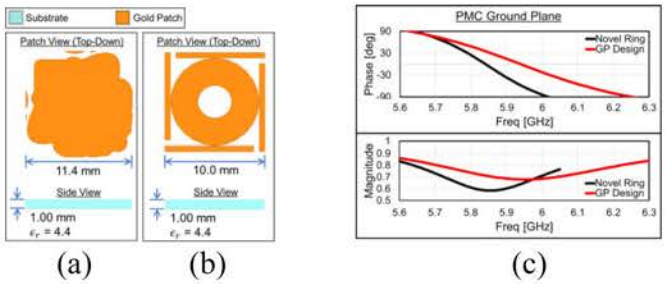

Fig. 1. (a) HGP AMC UC. (b) Novel ring AMC UC. (c) Reflection phase and magnitude of both UCs.

TABLE I
PERFORMANCE COMPARISON WITH NOVEL RING AMC

	Novel Ring	HGP Design
Center Freq. (GHz)	5.83	5.94
Min. Freq. (GHz)	5.64	5.63
Max. Freq. (GHz)	6.02	6.25
Bandwidth (%)	6.52	10.4
Min. Refl. Mag.	0.58	0.68

II. HYBRID GP METHOD

The HGP implemented is a tree-based GP that synthesizes and optimizes designs by first generating a random initial population of designs. The performance of each generated design is then evaluated via a cost function that is user-defined and varies depending on the design goal. After all members of the initial population are evaluated, the better performing designs go through mutation, crossover, or reproduction to produce the next generation. The process of mutation is to select part of the design and redesign it randomly. Crossover is when parts of two designs are selected and are swapped with one another. Reproduction is when a design in its entirety is passed on to the next generation. After a new generation is formed through the stated processes, the cycle is repeated till a design has been synthesized that meets all the desired design requirements.

The 2-D AMC ground planes are periodic structures. The HGP is used to generate the unit cells (UCs) of the metamaterials. The UCs consist of 2-D metallization patterns on a dielectric substrate with a PEC backing. For the design of tunable absorbers (which are also periodic structures), the 2-D UC patterns can be either metallization or electrostatically biased graphene.

The patterns in a UC are created by optimizing the number and the locations of vertices that, when connected, form 2-D areas of metallization or biased graphene. Each pattern's vertices can either be connected by a piecewise cubic spline or by straight lines. The 2-D patterns are allowed to extend from one UC into neighboring cells to achieve desired characteristics, e.g., lower resonant frequencies. The HGP also optimizes the number of metallization patterns for each AMC design. For tunable absorbers, the number as well as whether each pattern is metallization or biased graphene are optimized by the HGP. The 2-D patterns that are of the same material can be forced to separate or allowed to overlap. In the case where patterns are allowed to overlap, they are united and treated as a single new pattern. Vias are also included in the design variables, where the HGP can design and optimize via location and thickness. The HGP can also optimize the substrate thickness, UC size, and substrate material properties. Finally, the AMC ground plane UC designs can have four-fold rotational symmetry, reflection symmetry across the UC's diagonal, or enforcement of such symmetry could be ignored. The enforcement of symmetry lowers the polarization dependence [16], [20].

Four published designs are chosen for comparison to validate the HGP's performance. The AMC designs and the tunable THz absorber used for comparison are modeled in ANSYS's High Frequency Structure Simulator (HFSS). The AMC and absorber designs generated by the HGP are also modeled in HFSS. All designs generated by the HGP were constrained to use the same material properties for the dielectric substrate as the respective published design they are being compared with.

The cost function used to evaluate the performance of the AMC designs synthesized by the GP is as follows:

$$c = W_{\text{mag}} \sum_{i=1}^{N} -20\log_{10}|\Gamma_i| + W_{\text{phase}} \sum_{i=1}^{N} |\angle\Gamma_i| \quad (1)$$

where c is the cost, N is the number of frequencies the model is simulated at across the frequency range of interest, Γ_i is the reflection coefficient at the ith evaluated frequency, W_{mag} is the weight given to the magnitude of the reflection coefficient, and W_{phase} is the weight given to the phase of the reflection coefficient. The following is the cost function used to evaluate the tunable THz absorbers synthesized by the HGP

$$c = \sum_{i=1}^{N} |\Gamma_i|^2 \quad (2)$$

where c is the cost, N is the number of frequencies the model is simulated at across the frequency range of interest, and Γ_i is the reflection coefficient at the ith simulated frequency.

The criterion for the bandwidth of the AMC ground planes is that the reflection phase be within $\pm 90°$. The criterion for the bandwidth of the THz absorbers is that the absorption be equal to or greater than 80%.

For the purpose of reproduction, HFSS models of all the designs generated by the HGP can be found at http://hcac.hawaii.edu/HybridGPDesigns.zip. The HFSS models generated by HGP were run a second time to verify the results' stability. The second runs resulted in nearly identical results to the first runs. A test was also run to check the effects of fabrication errors. These tests showed that the HGP designs have low sensitivity to fabrication errors. The surface conductivity of graphene as a function of electrostatic bias is derived in [17].

III. RESULTS

A. Novel Ring AMC

The first AMC ground plane used for comparison comes from [18]. For convenience, this ground plane will be referred to as the novel ring AMC ground plane. Fig. 1(a) presents the AMC UC developed by the HGP. Fig. 1(b) presents the novel ring AMC UC in [18]. Fig. 1(c) presents the reflection phase and magnitude of the AMC generated by the HGP and the novel ring AMC. The HGP AMC is reflectively symmetric across the UC's diagonal and has no vias. The HGP was restricted to only generate substrates that are 1.00 mm thick and composed of FR-4.

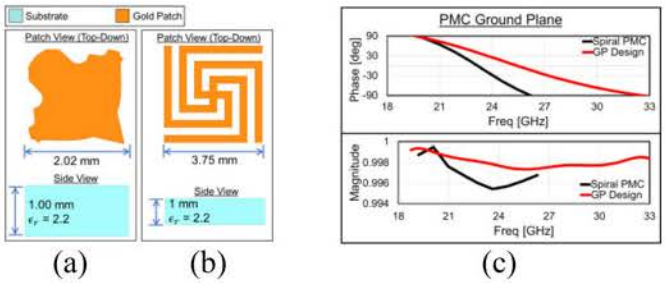

Fig. 2. (a) HGP AMC UC. (b) Spiral AMC UC. (c) Reflection phase and magnitude of both UCs.

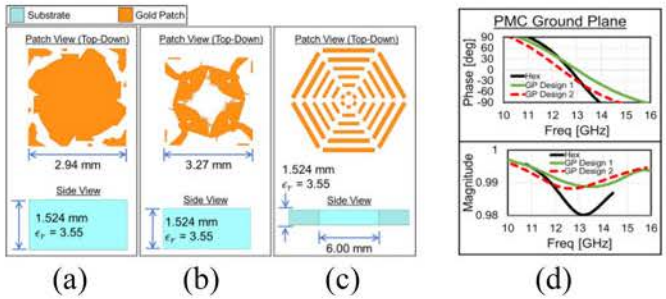

Fig. 3. HGP AMC UC. (a) Design 1. (b) Design 2. (c) Hexagonal AMC UC. (d) Reflection phase and magnitude of all UCs.

TABLE II
PERFORMANCE COMPARISON WITH SPIRAL AMC

	Spiral	HGP Design
Center Freq. (GHz)	23.0	26.1
Min. Freq. (GHz)	19.7	19.6
Max. Freq. (GHz)	26.2	32.5
Bandwidth (%)	28.3	49.4
Min. Refl. Mag.	1.00	1.00

TABLE III
PERFORMANCE COMPARISON WITH HEXAGONAL AMC

	Hexagonal	HGP Design 1	HGP Design 2
Center Freq. (GHz)	12.5	13.2	12.5
Min. Freq. (GHz)	11.0	10.6	10.3
Max. Freq. (GHz)	14.0	15.8	14.7
Bandwidth (%)	24.0	39.4	35.2
Min. Refl. Mag.	0.98	0.99	0.99

The AMC generated by the HGP's bandwidth is 60% larger and the minimum reflection magnitude is 17% larger than the novel ring AMC. Table I summarizes both AMCs' performances.

B. Spiral AMC

Next, the AMC ground plane used for performance comparison is a design presented in [19] referred to as the spiral AMC. Fig. 2(a) presents the AMC UC developed by the HGP. Fig. 2(b) presents the HFSS model of the spiral AMC UC in [19]. Fig. 2(c) presents the reflection phase and magnitude of the AMC generated by the HGP and the spiral AMC. The HGP AMC is reflectively symmetric across the UC's diagonal and has no vias. The HGP was restricted so that only substrates that were 1.00 mm thick and having a relative permittivity of 2.2 were generated.

The AMC generated by the HGP's bandwidth is 74.6% larger and the minimum reflection magnitude is equal compared with the spiral AMC. Table II summarizes both AMCs' performances.

C. Hexagonal AMC

Now, we will look at an AMC used for performance comparison presented in [20], which will be referred to as the hexagonal AMC. The HGP was run twice to generate two separate designs. Fig. 3(a) presents the AMC UC developed by the first run of the HGP, whereas Fig. 3(b) presents the AMC UC developed by the second run. Fig. 3(c) presents the hexagonal AMC UC, and Fig. 3(d) shows the reflection phase and magnitude of the AMCs generated by the HGP and the hexagonal AMC. The HGP AMCs have four-fold rotational symmetry and have no vias. The HGP was restricted so that all generated designs' substrates were 1.524 mm thick and were composed of Rogers RO4003C.

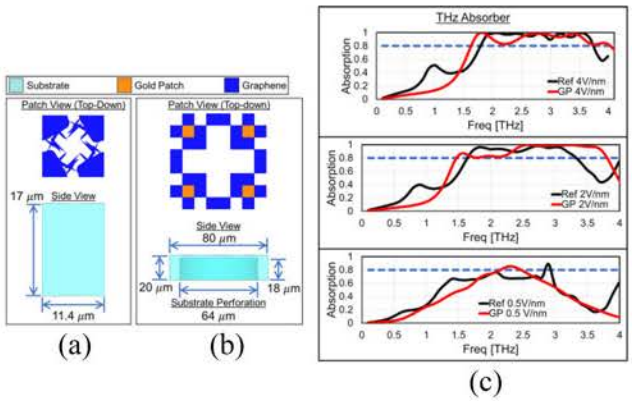

Fig. 4. (a) HGP absorber UC. (b) Pixelated absorber UC. (c) Absorption of both UCs when bias is 4, 2, and 0.5 V/nm.

The AMCs generated by the HGP's bandwidths are 73.3% and 46.7% larger and the minimum reflection magnitudes are both 1.0% larger for HGP Design 1 and Design 2, respectively. The two HGP designs show that the HGP produces significantly different UC designs when run a second time. By having several UC designs optimized for the same operating frequency, deeper insights can be gained about the cause that leads the HGP designs to the larger bandwidths. The two HGP designs have slightly different bandwidths, while both outperform the reference design. Table III summarizes the performance of the hexagonal AMC and the AMCs generated by the HGP.

D. Tunable THz Absorber

The absorber used for comparison is presented in [15]. For convenience of discussion, this absorber design will be referred to as the pixelated absorber. The UC design that the HGP synthesized and the pixelated absorber UC can be seen in Fig. 4(a)

TABLE IV
PERFORMANCE COMPARISON WITH PIXELATED ABSORBER

4 V/nm	Pixelated	HGP Design
Center Freq. (THz)	2.77	2.83
Min. Freq. (THz)	1.79	1.63
Max. Freq. (THz)	3.74	4.03
Bandwidth (%)	70.4	84.8
2 V/nm	Pixelated	HGP Design
Center Freq. (THz)	2.49	2.64
Min. Freq. (THz)	1.64	1.47
Max. Freq. (THz)	3.34	3.81
Bandwidth (%)	68.3	88.6

and (b), respectively. Fig. 4(c) presents the absorption of the HGP absorber and the pixelated absorber when the bias is 4, 2, and 0.5 V/nm. The HGP absorber has four-fold rotational symmetry, no via, and no metallization. The HGP was restricted so that the substrate could only be 18 μm thick or less and so that the substrate had a relative permittivity of either $\varepsilon_r = 4$ or $\varepsilon_r = 3.5 + 0.2j$ as implemented in [15].

When the bais is 4 V/nm, the bandwidth of the HGP absorber is 23.1% larger than the pixelated absorber. For a bias of 2 V/nm, the HGP absorbers bandwidth is 37.6% larger, and for a bias of 0.5 V/nm, the bandwidth is 400% larger. Table IV summarizes the performance of the pixelated absorber and the HGP absorber when the bias is 4, 2, and 0.5 V/nm.

IV. CONCLUSION

An HGP code was further developed to include the added functionality of synthesizing 2-D AMC ground planes and tunable THz absorbers. The added functionality's performance has been validated by comparing the UC designs generated by the HGP with three existing published AMC ground planes and a tunable THz absorber. The results show that the HGP produces human-competitive results and can produce high-gain low-profile wideband AMC ground planes in the 2-D design space. The HGP designed AMCs have bandwidths that range from 60% to 74.6% larger than that of the reference AMCs while maintaining reflection magnitudes that are equal to or up to 17% larger than that of the reference AMCs. The 2-D AMC ground planes designed by the HGP are an attractive option, compared with 3-D designs reported earlier as they provide low-profile antennas and other microwave device designs an option that has relative ease and low cost of fabrication, in addition to improved performance, including wider bandwidth and increased reflection coefficient. The results of the tunable THz absorber show that the HGP can produce wider bandwidth absorbers than other nature-inspired techniques with bandwidths that range from 23.1% to 400% larger than the reference absorber design.

Future work includes furthering the understanding of the electromagnetic characteristics of the unconventional and complex topology of UC designs synthesized by the HGP. Equivalent circuit models are being developed and validated for these designs. The equivalent circuit models will give insight into how these designs and complex topologies are behaving and in fact are outperforming designs based on conventional human expertise. Prony's method will also be implemented to find the complex natural resonance frequencies giving insight into how the HGP designs have wider bandwidths.

REFERENCES

[1] C. Caloz and T. Itoh, *Electromagnetic Metamaterials*, 1st ed., N. J. Hoboken, Ed. Hoboken, NJ, USA: Wiley, 2005, pp. 1–2.

[2] H. Tao, N. Landy, C. Bingham, X. Zhang, R. Averitt, and W. Padilla, "A metamaterial absorber for the terahertz regime: Design, fabrication and characterization," *Opt. Express*, vol. 16, no. 10, pp. 7181–7188, 2008.

[3] Q. Wen, H. Zhang, Y. Xie, Q. Yang, and Y. Liu, "Dual band terahertz metamaterial absorber: Design, fabrication, and characterization," *Appl. Phys. Lett.*, vol. 95, no. 24, 2009, Art. no. 241111.

[4] S. Kuznetsov, A. Paulish, A. Gelfand, P. Lazorskiy, and V. Fedorinin, "Matrix structure of metamaterial absorbers for multispectral terahertz imaging," *Prog. Electromagn. Res.*, vol. 122, pp. 93–103, 2012.

[5] N. I. Landy, S. Sajuyigbe, J. J. Mock, D. R. Smith, and W. J. Padilla, "A perfect metamaterial absorber," *Phys. Rev. Lett.*, vol. 100, no. 20, 2008, Art. no. 207402.

[6] N. Liu, M. Mesch, T. Weiss, M. Hentschel, and H. Giessen, "Infrared perfect absorber and its application as plasmonic sensor," *Nano Lett.*, vol. 10, no. 7, pp. 2342–2348, 2010.

[7] K. Iwaszczuk, A. Strikwerda, K. Fan, X. Zhang, R. Averitt, and P. Jepsen, "Flexible metamaterial absorbers for stealth applications at terahertz frequencies," *Opt. Express*, vol. 20, no. 1, pp. 635–643, 2011.

[8] R. Kakimi, M. Fujita, M. Nagai, M. Ashida, and T. Nagatsuma, "Capture of a terahertz wave in a photonic-crystal slab," *Nature Photon.*, vol. 8, no. 8, pp. 657–663, 2014.

[9] D. Kern, M. Wilhelm, D. Werner, and P. Werner, "A novel design technique for ultra-thin tunable EBG AMC surfaces," in *Proc. IEEE Antennas Propag. Soc. Symp.*, 2004, pp. 1167–1170.

[10] Z. Bayraktar, J. Bossard, and D. Werner, "AMC metamaterials for low-profile antennas mounted on or embedded in composite platforms," in *Proc. IEEE Antennas Propag. Int. Symp.*, 2007, pp. 1305–1308.

[11] D. Kern, D. Werner, A. Monorchio, L. Lanuzza, and M. Wilhelm, "The design synthesis of multiband artificial magnetic conductors using high impedance frequency selective surfaces," *IEEE Trans. Antennas Propag.*, vol. 53, no. 1, pp. 8–17, Jan. 2005.

[12] L. Deias, G. Mazzarella, and N. Sirena, "EBG substrate synthesis for 2.45 GHz applications using genetic programming," in *Proc. IEEE Antennas Propag. Soc. Int. Symp.*, 2010, pp. 1–4.

[13] J. Rayno, M. Iskander, and N. Celik, "Synthesis of broadband true-3D metamaterial artificial magnetic conductor ground planes using genetic programming," *IEEE Trans. Antennas Propag.*, vol. 62, no. 11, pp. 5732–5744, Nov. 2014.

[14] J. Rayno, M. Iskander, and M. Kobayashi, "Hybrid genetic programming with accelerating genetic algorithm optimizer for 3-D metamaterial design," *IEEE Antennas Wireless Propag. Lett.*, vol. 15, pp. 1743–1746, 2016.

[15] E. Torabi, A. Fallahi, and A. Yahaghi, "Evolutionary optimization of graphene-metal metasurfaces for tunable broadband terahertz absorption," *IEEE Trans. Antennas Propag.*, vol. 65, no. 3, pp. 1464–1467, Mar. 2017.

[16] A. Andryieuski and A. Lavrinenko, "Graphene metamaterials based tunable terahertz absorber: Effective surface conductivity approach," *Opt. Express*, vol. 21, no. 7, pp. 9144–9155, 2013.

[17] G. Hanson, "Dyadic green's functions for an anisotropic, non-local model of biased graphene," *IEEE Trans. Antennas Propag.*, vol. 56, no. 3, pp. 747–757, Mar. 2008.

[18] M. Xie, Q. Guo, and K. Huang, "Design of a novel artificial magnetic conductor plane and its application for low-profile dipole," in *Proc. Int. Conf. Microw. Millim. Wave Technol.*, 2010, pp. 2085–2087.

[19] Y. Kim, F. Yang, and A. Elsherbeni, "Compact artificial magnetic conductor designs using planar square spiral geometries," *Prog. Electromagn. Res.*, vol. 77, pp. 43–54, 2007.

[20] M. de Cos, Y. Alvarez, and F. Las-Heras, "Novel broadband artificial magnetic conductor with hexagonal unit cell," *IEEE Antennas Wireless Propag. Lett.*, vol. 10, pp. 615–618, 2011.